PRIMARY RESEARCH ARTICLE

The response of stomatal conductance to seasonal drought in tropical forests

Jin Wu[1,2] | Shawn P. Serbin[1] | Kim S. Ely[1] | Brett T. Wolfe[3] | L. Turin Dickman[4] | Charlotte Grossiord[4] | Sean T. Michaletz[4] | Adam D. Collins[4] | Matteo Detto[3,5] | Nate G. McDowell[4] | S. Joseph Wright[3] | Alistair Rogers[1]

[1]Environmental & Climate Sciences Department, Brookhaven National Laboratory, Upton, NY, USA

[2]School of Biological Sciences, University of Hong Kong, Pokfulam, Hong Kong

[3]Smithsonian Tropical Research Institute, Apartado, Panama

[4]Earth and Environmental Sciences Division, Los Alamos National Laboratory, Los Alamos, NM, USA

[5]Ecology and Evolutionary Biology Department, Princeton University, Princeton, NJ, USA

Correspondence
Jin Wu, School of Biological Sciences, University of Hong Kong, Pokfulam, Hong Kong.
Email: jinwu@hku.hk

Present address
Sean T. Michaletz, Department of Botany and Biodiversity Research Centre, University of British Columbia, Vancouver, BC V6T 1Z4, Canada

Nate G. McDowell, Pacific Northwest National Laboratory, Richland, WA 99354, USA

Abstract

Stomata regulate CO_2 uptake for photosynthesis and water loss through transpiration. The approaches used to represent stomatal conductance (g_s) in models vary. In particular, current understanding of drivers of the variation in a key parameter in those models, the slope parameter (i.e. a measure of intrinsic plant water-use-efficiency), is still limited, particularly in the tropics. Here we collected diurnal measurements of leaf gas exchange and leaf water potential (Ψ_{leaf}), and a suite of plant traits from the upper canopy of 15 tropical trees in two contrasting Panamanian forests throughout the dry season of the 2016 El Niño. The plant traits included wood density, leaf-mass-per-area (LMA), leaf carboxylation capacity ($V_{c,max}$), leaf water content, the degree of isohydry, and predawn Ψ_{leaf}. We first investigated how the choice of four commonly used leaf-level g_s models with and without the inclusion of Ψ_{leaf} as an additional predictor variable influence the ability to predict g_s, and then explored the abiotic (i.e. month, site-month interaction) and biotic (i.e. tree-species-specific characteristics) drivers of slope parameter variation. Our results show that the inclusion of Ψ_{leaf} did not improve model performance and that the models that represent the response of g_s to vapor pressure deficit performed better than corresponding models that respond to relative humidity. Within each g_s model, we found large variation in the slope parameter, and this variation was attributable to the biotic driver, rather than abiotic drivers. We further investigated potential relationships between the slope parameter and the six available plant traits mentioned above, and found that only one trait, LMA, had a significant correlation with the slope parameter ($R^2 = 0.66$, $n = 15$), highlighting a potential path towards improved model parameterization. This study advances understanding of g_s dynamics over seasonal drought, and identifies a practical, trait-based approach to improve modeling of carbon and water exchange in tropical forests.

KEYWORDS
carbon and water exchange, leaf age, leaf water potential, plant traits, spectroscopy, stomatal conductance model, stomatal slope, vulnerability curve

1 | INTRODUCTION

Stomata regulate the exchange of carbon and water between plants and the atmosphere (Cowan & Farquhar, 1977; Lawson & Vialet-Chabrand, 2018; Sperry et al., 2017). At large scales, control of stomatal aperture regulates regional and global biogeochemical cycles of carbon, water and energy, and influences the climate through vegetation-mediated climate feedbacks (Bonan, 2008; Pielke et al., 1998; Zeng et al., 2017). Therefore, the representation of stomatal conductance (g_s) is a fundamental component of Terrestrial Biosphere Models (TBMs), and is essential to formulate correctly because it also captures the impacts of ongoing global change on the climate system.

Four previously developed and widely used leaf-level models of g_s have been adopted by current TBMs. These include the phenomenological Ball–Berry (BB; Ball, Woodrow, & Berry, 1987), Ball–Berry–Katul (BBK; Katul, Manzoni, Palmroth, & Oren, 2010), and Ball–Berry–Leuning (BBL; Leuning, 1995) models, and the optimality-based unified stomatal optimization model (USO; Medlyn et al., 2011). The phenomenological models are based on empirical observations of stomatal behavior in response to environmental stimuli, whereas the optimality model is based on the principle that stomata act to maximize carbon gain while minimizing water loss (Cowan & Farquhar, 1977). Among these models, the BB and BBK formulations use relative humidity (RH) while the BBL and USO formulations represent g_s responses to vapor pressure deficit (D). Although D-type models more closely reflect stomatal mechanics and are directly proportional to water loss (e.g. Aphalo & Jarvis, 1991; Eamus, Taylor, Macinnis-NG, Shanahan, & de Silva, 2008), both RH-type and D-type g_s models are still widely used in TBMs (e.g. Franks et al., 2018; Knauer et al., 2017; Rogers, Medlyn, et al., 2017). Moreover, the performance of RH-type and D-type models has rarely been evaluated in natural forests across diverse species with in-situ gas exchange measurements, particularly in tropical forest biomes where changes in RH and D are typically tightly coupled. Despite these fundamental differences, phenomenological and optimality-based g_s models are structurally similar (Medlyn et al., 2011) and they generate comparable g_s predictions under many biotic and abiotic conditions (Sperry et al., 2017). Common to all these models is a representation of g_s that varies approximately linearly with net CO_2 assimilation rate (A) for a given set of environmental conditions (temperature, humidity and leaf-surface CO_2 concentration). Therefore, the slope parameter of this coupled g_s–A relationship, which is an indicator of intrinsic plant water use efficiency (referring to the amount of water release through stomata for given A and environmental conditions as shown in Figure 1), is fundamental to all these models.

Although it has been shown that the value of the slope parameter can have a large impact on simulated carbon and water fluxes (Bauerle, Daniels, & Barnard, 2014; Franks et al., 2018; Jefferson, Maxwell, & Constantine, 2017), our understanding of the variability in the slope parameter is far from complete. Particularly, it is unclear what drives variation in the slope parameter, which has been shown to change with both biotic (i.e. tree-species identification

and associated leaf characteristics) and abiotic factors (i.e. growth environment, and seasonal and inter-annual environmental variability such as drought and warming; e.g. Heroult, Lin, Bourne, Medlyn, & Ellsworth, 2013; Lin et al., 2015; Medlyn et al., 2011; Pantin, Simonneau, & Muller, 2012; Wolz, Wertin, Abordo, Wang, & Leakey, 2017). This lack of a clear understanding of the impact of biotic and abiotic controls on the slope parameter has contributed to the current controversy on the choice of the most appropriate and parsimonious formulation of g_s models to implement in TBMs. For example, recent experimental and seasonal drought-based studies have shown that the abiotic control of the slope parameter can be as important as the biotic control, especially under soil moisture stress (e.g. Drake et al., 2017; Heroult et al., 2013; Zhou et al., 2014). This can arise either from the shorter timescale (e.g. diurnal) coordinated variation between leaf water potential and D (Anderegg et al., 2017), from the increasing soil moisture stress that can induce the associated change in plant water potential
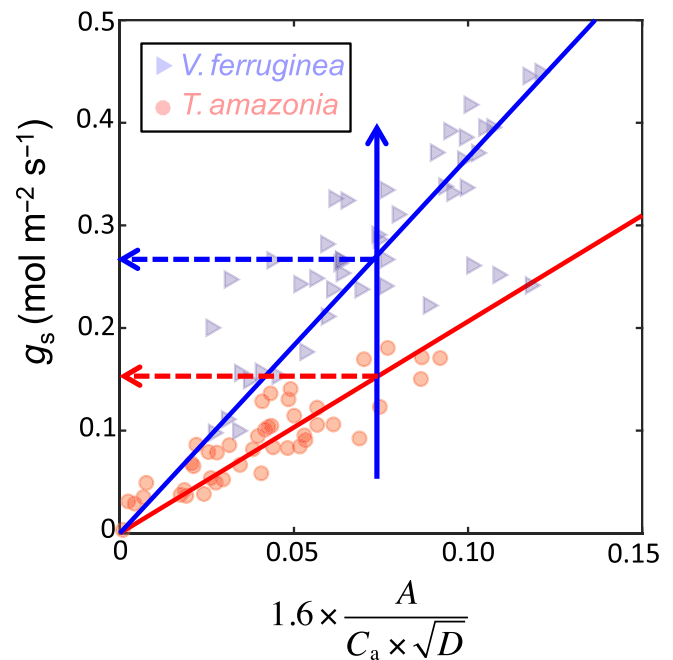
FIGURE 1 The slope parameter of the unified stomatal optimization model (USO; Medlyn et al., 2011) is an indicator of intrinsic water use efficiency. The regression slope between stomatal conductance (g_s) and the USO model index $\left(1.6 \times \left(A / \left(C_a \times \sqrt{D}\right)\right)\right)$ shown below is almost linearly proportional to the stomatal slope of the USO model (see Figure S1). For a given CO_2 assimilation rate (A), atmospheric CO_2 concentration (C_a), and leaf-to-air vapor pressure deficit (D) a higher regression slope (and thus stomatal slope) means that plants maintain a higher g_s to keep the same photosynthetic rate. As such, the stomatal slope parameter is an indicator of intrinsic plant water use efficiency, and a greater stomatal slope equates to a lower intrinsic water use efficiency. The background scatterplots include diurnal gas exchange measurements for two example tree-species (*Vochysia ferruginea*, blue and *Terminalia amazonia*, red) at the San Lorenzo site in Panama (see Table 1 for more details), and the regression coefficients and model performance were summarized in Table 2

which down-regulates g_s and thus the slope parameters (e.g. Drake et al., 2017; Heroult et al., 2013; Zhou et al., 2014), or there is coordinated acclimation of the slope parameter with seasonal variation in soil moisture and plant water potential (e.g. Koepke & Kolb, 2012; Xu & Baldocchi, 2003). Regardless of the reasons, the inclusion of a plant or leaf water potential variable with the original g_s formulations has recently been increasingly advocated as a way to improve prediction of g_s (Anderegg et al., 2017; Drake et al., 2017; Zhou et al., 2014). Despite the recommendation of these previous studies, it remains unclear whether these results are representative of wider natural plant communities, and importantly, systems such as the tropics where tall canopy evergreen trees have evolved root systems to adapt to seasonal variability in soil moisture content (Giardina et al., 2018; Meinzer et al., 1999).

Although large variability in the slope parameter has been previously observed within and across biomes (Dietze et al., 2014; Lin et al., 2015), many TBMs use just two slope parameters to differentiate between vegetation with the C3 and C4 photosynthetic pathways (e.g. Kowalczyk et al., 2006; Oleson et al., 2013; Sitch et al., 2003). Other TBMs incorporate additional slope values for different plant functional types (PFTs), for example needleleaf evergreen trees, broadleaf deciduous trees and C3 crops (Baldocchi & Meyers, 1998; Oleson et al., 2010), or by using different slope parameters for temperate and tropical plants (Medvigy, Wofsy, Munger, Hollinger, & Moorcroft, 2009). While past efforts to define the values of stomatal slope across different PFTs were limited by data, recent syntheses and analyses have provided improved understanding of global-scale variation in the slope parameter, enabling the data-driven parameterization of stomata control in up to 10 different global PFTs (Lin et al., 2015; Miner, Bauerle, & Baldocchi, 2017).

Tropical forests account for around one-third of annual terrestrial photosynthesis (Beer et al., 2010), and, through stomatal control of transpiration, mediate tropical convection and the timing of dry-to-wet season transitions—a potentially important climate feedback (Wright et al., 2017). However, for such a globally important and hyperdiverse biome, typically only one value for the slope parameter is assigned in current TBMs (Lin et al., 2015; Miner et al., 2017; Rogers, Medlyn, et al., 2017). One approach to improve the representation of stomatal response in TBMs is to establish empirical relationships between the slope parameter and other plant traits (e.g. Lin et al., 2015). Not only do such relationships provide an empirical way to link plant traits to the variability in the slope parameter within vegetation communities (Xu, Medvigy, Powers, Becknell, & Guan, 2016), but they might also elucidate the biological mechanisms underlying such variability (Lin et al., 2015). However, whether the previously observed global-scale relationships between the slope parameter and key plant traits as shown in Lin et al. (2015) also holds within forest communities, that is, across tropical tree-species and forest sites, remains uncertain.

The goal of this study was to identify the best potential model representation, and explore the underlying ecological understanding, of the response of g_s to seasonal drought in tropical forests. Specifically, we examined the impact of stomatal model choice (i.e. BB, BBK, BBL or USO), inclusion of leaf water potential (Ψ_{leaf}), as well as abiotic and biotic drivers of variation in the slope parameter on the ability to predict g_s dynamics in the tropics. We collected a unique field dataset consisting of fifteen evergreen tree-species in two forests over the course of the 2016 dry season, which due to a strong 2015–2016 El Niño event (Liu et al., 2017) was drier than the historical mean. Since both growth environment and leaf phenology might affect stomatal response to diurnal and seasonal environmental variability, here we aim to first standardize these effects by focusing solely on canopy-top, sunlit leaves at their fully mature status. By controlling the leaf age variation in this way together with environmental variability captured by the g_s models, the primary abiotic drivers of the slope parameter that we considered included forest sites and the month of measurement (which represented seasonal variability in soil moisture content and atmospheric humidity). The biotic factors included tree-species specific response and their associated plant traits, which are either mechanistically or phenomenologically linked to photosynthesis or transpiration (e.g. Wright et al., 2004; Xu et al., 2016). The six plant traits we considered include wood density, leaf-mass-per-area (LMA), leaf carboxylation capacity ($V_{c,max25}$), leaf water content, the degree of isohydry (Martinez-Vilalta, Povatos, Aguadé, Retana, & Mencuccini, 2014), and predawn Ψ_{leaf}. We asked four questions: (a) Does the inclusion of Ψ_{leaf} as an additional predictor variable improve the simulation of g_s of tropical trees? (b) Which model formulation best captures observed g_s? (c) How do abiotic and biotic drivers of variation in the slope parameter influence the ability to predict g_s? (d) Are there any key relationships with plant traits, particularly those widely observed or easily measured, that could be used to constrain variation in the slope parameter within models? Through answering these questions, we aim to improve understanding of g_s dynamics in tropical forests, and potentially provide a practical approach to advance TBM representation of g_s, thereby enabling a more accurate representation of carbon and water dynamics in tropical ecosystems.

2 | MATERIALS AND METHODS

2.1 | Sites and materials

This study was conducted at two lowland tropical moist forest sites separated by 80 km on opposite sides of the Isthmus of Panama. At each site, the Smithsonian Tropical Research Institute maintains a canopy-access crane that enables access to the forest canopy. These sites include a seasonally dry forest in the Parque Natural Metropolitano (PNM; 8°59′41.55″N, 79°32′35.22″W) near Panama City and a wet evergreen forest in the San Lorenzo Protected Area (SLZ; 9°16′51.71″N, 79°58′28.27″W), Colon Province. Historic (1998–2015) mean annual air temperature is 26.3°C and 25.8°C, and mean annual precipitation is 1,826 and 3,286 mm for PNM and SLZ, respectively, with ~90% of the rainfall in the May–December wet season (Figure 2). For more details on these sites see Wright et al. (2003).
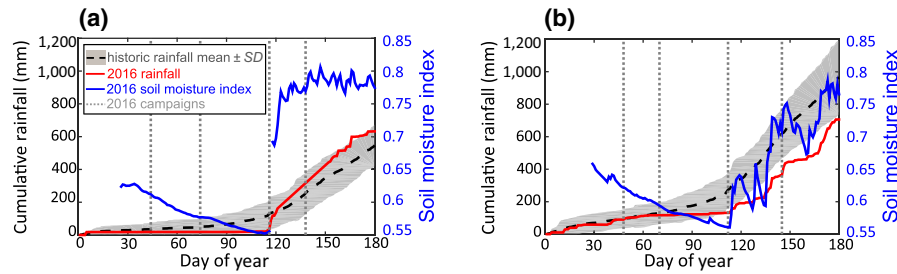
(a) **(b)**

FIGURE 2 Four field campaigns were conducted in each of the two Panamanian crane sites in 2016. These are (a) the Parque Natural Metropolitano crane site (PNM) and (b) the San Lorenzo crane site (SLZ). Campaigns included diurnal measurements of gas exchange, leaf water potential and leaf traits. The rainfall data for historic (1998–2015; black broken line) and 2016 (red line) trends were obtained from biogeodb.stri.si.edu/physical_monitoring; the shading indicates one standard deviation (std) of the historic mean. The soil moisture index (blue line) measures the relative soil water content, where 1 = fully saturated soil. The soil moisture index was calculated using a daily integrated value, and was obtained by averaging soil moisture values across three different soil depths (at 10, 40, and 100 cm) and time (at 5 min interval across the day), divided by the maximum value in the record

Fifteen evergreen canopy tree-species with no within species replication ($n = 7$ for PNM and $n = 8$ for SLZ; Table 1) were selected for intensive field measurements of leaf gas exchange and plant traits. These tree species were within the canopy crane access footprint and were selected to capture the diversity of tree species and plant trait space present at each site. In order to minimize the effects of leaf phenology and canopy environments on variation in field-measured stomatal conductance, we restricted measurements to current-season, fully-expanded, upper canopy sunlit foliage. We conducted four campaigns in 2016 at monthly intervals from mid-February until mid-May, covering the middle of dry-season to the beginning of wet-season (Figure 2; Figure S2). We spent 2 days at each location each month and conducted diurnal measurements of leaf gas exchange and leaf water potential (Ψ_{leaf}), measured photosynthetic CO_2 response curves and collected additional leaf traits. The May campaign had a reduced scope and only focused on measurements of diurnal leaf gas exchange and Ψ_{leaf}.

2.2 | Measurements of leaf gas exchange and traits

We used six portable gas exchange systems (LI-6400XT, LI-COR Inc.) equipped with a 2×3 cm^2 leaf chamber and red-blue light source. These gas exchange systems were zeroed with a common nitrogen standard prior to each campaign. Diurnal leaf gas exchange measurements were made in-situ using cranes to access the canopy throughout the day. Each tree-species was measured five to seven times per day, and at each time point two leaves were measured and then harvested for subsequent trait measurements. Measurements of diurnal gas exchange, including A, g_s, leaf surface CO_2 concentration (C_a), intercellular CO_2 concentration (C_i), RH, leaf-to-air vapor pressure deficit (D) and leaf temperature, followed the method of Bernacchi et al. (2006), and were used to evaluate leaf level g_s models (see below). Prior to the gas exchange measurements, the temperature of each measured leaf was recorded, and chamber conditions were matched to the ambient environment. For each measurement round (time point), the sample chamber temperature (T_{block}) was set to the ambient air temperature. For each tree, the sample chamber light was set to the photosynthetically active radiation incident on the leaf. This was adjusted throughout each measurement time point to account for changing light conditions due to intermittent cloud cover and leaf aspect. For each tree-species, chamber CO_2 concentration was set to ambient CO_2 concentration plus the differential expected due to CO_2 assimilation. The RH of the air entering the leaf chamber was not reduced so as to keep it close to ambient conditions. A high flow rate (500 μmol/s) was used to minimize the time taken for A and g_s to stabilize. After clamping in the chamber, rates were monitored using the instrument's graphical interface and statistical output, and data logged after A and g_s reached stability. To ensure we were capturing gas exchange rates representative of ambient conditions data were logged within a maximum of 90 s after clamping the leaf in the measurement chamber.

Over the course of the season we made c. 46 measurements per tree-species for a total 694 individual measurements. Prior to data analysis we filtered our initial dataset of survey measurements by removing spurious data (e.g. negative values) and data where we believed values were not reliable due to a mismatch between sample and reference IRGAs, or where measured values indicated an artifact (e.g. dew on the leaves early in the morning, or poor contact with the leaf thermocouple) or poor replication of ambient conditions. These data were identified by flagging data where the C_i:C_a ratio was <0.2 or >0.9, or where RH was <35% or >90%. Following examination of these flagged data records 83% of the total dataset remained and was used for subsequent analysis.

Measurement of the response of A to C_i, commonly known as A–C_i curves, was conducted on detached branch sections. All branches were sampled before dawn using the canopy crane. We took steps to protect the samples from xylem embolism, and where possible branches were cut underwater by bending the branch into a bucket filled with water. In all cases >1 m of branch was removed within 15 min of the initial cut by recutting the branch section underwater in a large container. Samples were stored in individual buckets and kept in deep shade until used for measurements. Measurement of A–C_i curves closely followed the approach recently described by

TABLE 1 Species, canopy status and plant traits (mean ± standard deviation) for all tree-species sampled at the two crane sites (the PNM site, and the SLZ site) in Panama

Site	Species	Family	Height (m)	DBH (cm)	LMA (g/m²)	LWC (%)	$V_{c,max25}$ (μmol m⁻² s⁻¹)	Wood density (g/cm³)	Predawn Ψ_{leaf} (MPa)	Degree of iso-hydry (slope of predawn Ψ_{leaf}: mid-day Ψ_{leaf})	Stem vulnerability curve parameter b	Stem vulnerability curve parameter c
PNM	Albizia adinocephala	Fabaceae	29.4	29.5	89 ± 11	48 ± 5	53 ± 10	N/A	−1.9 ± 0.5	1.96	1.3 ± 0.3	2.8 ± 1.6
PNM	Pittoniotis trichantha	Rubiaceae	19	21.0	91 ± 16	53 ± 5	31 ± 2	0.60	−1.0 ± 0.4	1.46	1.9 ± 0.5	10.3 ± 21.3
PNM	Calycophyllum candidissimum	Rubiaceae	20.1	39.5	92 ± 9	56 ± 4	44 ± 23	0.75	−1.4 ± 0.8	1.02	1.7 ± 15.8	15.8 ± 824.9
PNM	Castilla elastica	Moraceae	23.5	38.0	102 ± 5	58 ± 2	46 ± 13	0.34	−1.0 ± 0.4	0.48	1.3 ± 0.6	2.0 ± 2.1
PNM	Cordia alliodora	Boraginaceae	22	28.3	92 ± 11	53 ± 4	75 ± 6	0.46	−1.7 ± 0.3	0.78	3.3 ± 1.7	6.1 ± 13.9
PNM	Ficus insipida	Moraceae	31.2	95.4	119 ± 14	65 ± 3	78 ± 10	0.34	−1.4 ± 0.3	−0.21	1.0 ± 11.6	1.2 ± 15.9
PNM	Luehea seemannii	Tiliaceae	26	63.2	147 ± 11	47 ± 2	85 ± 8	0.57	−1.4 ± 0.6	0.52	3.0 ± 2.0	10.8 ± 29.1
SLZ	Carapa guianensis	Meliaceae	33.9	62.0	152 ± 16	52 ± 4	25 ± 4	0.55	−0.8 ± 0.2	0.19	1.3 ± 0.5	21.4 ± 119.9
SLZ	Guatteria dumetorum	Annonaceae	35	59.0	84 ± 7	55 ± 5	35 ± 4	0.45	−1.1 ± 0.6	0.04	1.3 ± 0.6	2.1 ± 1.4
SLZ	Miconia borealis	Melastomatac	24.8	34.0	99 ± 9	51 ± 3	59 ± 1	N/A	−1.6 ± 0.7	0.37	1.6 ± 0.8	1.5 ± 1.1
SLZ	Tachigali versicolor	Fabaceae	30.4	57.4	95 ± 10	46 ± 4	36 ± 4	0.58	−1.2 ± 0.5	0.47	0.8 ± 1.2	1.1 ± 1.3
SLZ	Terminalia amazonia	Combretaceae	27	52.9	131 ± 13	52 ± 4	47 ± 16	0.67	−0.9 ± 0.3	1.32	1.2 ± 0.4	2.0 ± 1.6
SLZ	Tocoyena pittieri	Rubiaceae	26.6	53.3	93 ± 10	62 ± 3	38 ± 6	0.64	−0.9 ± 0.4	0.53	3.6 ± 2.0	4.0 ± 7.3
SLZ	Virola multiflora	Myristicacea	22.7	35.1	154 ± 10	55 ± 3	18 ± 1	0.45	−0.9 ± 0.5	0.19	1.4 ± 0.4	3.9 ± 4.4
SLZ	Vochysia ferruginea	Vochysiaceae	29.4	58.0	114 ± 11	61 ± 4	51 ± 14	0.39	−0.8 ± 0.3	0.38	1.0 ± 0.3	3.5 ± 3.4

Abbreviations: DBH, diameter at breast height; LMA, leaf-mass-per-area; LWC, leaf water content; PNM, Parque Natural Metropolitano; SLZZ, San Lorenzo.

Rogers, Serbin, Ely, Sloan, and Wullschleger (2017). Apparent maximum photosynthetic capacity standardized to a reference temperature of 25°C ($V_{c,max25}$) was estimated using the kinetic constants and temperature response functions presented by Bernacchi et al. (2013) as described by Rogers, Serbin, et al. (2017). A total of 120 estimates of $V_{c,max25}$ were used in this study (c. 8 per tree-species), with tree-species-specific mean and standard deviation summarized in Table 1.

Following in-situ gas exchange measurement, the leaves were immediately harvested for Ψ_{leaf} and trait measurement. Leaves were sealed in humidified plastic bags and stored in the dark on ice for a maximum of two hours before further processing. Ψ_{leaf} was measured using a Scholander-type pressure chamber (PMS) as described previously (McDowell, Brooks, Fitzgerald, & Bond, 2003). We also tested the robustness of our methodology used to measure Ψ_{leaf} through an experimental test by examining the impact of the time duration of wait time prior to measurement on the Ψ_{leaf} observed, and the results showed that within the 2-hr, leaf storage in the dark on ice had little impact on the estimated Ψ_{leaf}. These experimental results are summarized in Methods S1 and Figure S3. We then sampled a known leaf area using cork borers and weighed leaf fresh mass with a precision balance (Fisher Science Education, Model SLF303). Once weighed, the samples were dried to constant mass at 70°C. We then determined dry mass to calculate LMA (g/m^2) and leaf water content (LWC; as a percentage of fresh mass, %). We also collected leaf samples (2–3 replicates per tree-species per campaign) before dawn to measure pre-dawn Ψ_{leaf}. Based on the predawn and diurnal measurements of Ψ_{leaf}, we derived a tree-species-specific plant hydrological trait, degree of isohydry, which is defined by the slope of pre-dawn and mid-day Ψ_{leaf}, following the approach as Martinez-Vilalta, Povatos, Aguadé, Retana, and Mencuccini (2014). In addition, we used the existing data on stem wood density for our target tree-species collected from the same forests (Wright et al., 2010). Canopy height and diameter at breast height for the target tree-species referred to Dickman et al. (2019).

Independent of the diurnal measurement campaigns, for the same tree-species at each site, we also measured stem hydraulic conductivity as a function of stem water potential (i.e. hydraulic vulnerability curves) in terminal branches of canopy trees. Following the approach described by Wolfe, Sperry, and Kursar (2016), we measured hydraulic conductivity on 20–52 stem segments per tree-species (mean stem diameter = 5.9 mm) that had been air dried to reach varying stem water potential. For each tree-species, stem hydraulic conductivity was plotted as a function of stem water potential and a Weibull function was fit through the 90th percentile to obtain the vulnerability curve parameters (summarized in Table 1).

We recognize that there are alternative approaches to deriving fitted parameters and additional value in many of the traits we have collected. Therefore, all the data associated with this study including raw gas exchange data, fitted photosynthetic parameters and leaf trait are publicly available at the NGEE-Tropics dataset archive (Ely et al., 2018a, 2018b; Rogers et al., 2018a, 2018b; Wolfe et al., 2018),

the TRY database (Kattge et al., 2011) and the database (www. BETYd.org) associated with the PEcAn project (LeBauer et al., 2018).

2.3 | Stomatal conductance models

We utilized the four common models to describe the coupled g_s–A relationship to environmental variables, including BB, BBK, BBL and USO (as described in the Introduction).

The BB model (Ball et al., 1987) is formulated as follows:

$$g_s = g_0 + m \times \frac{A \times RH}{C_a}, \tag{1}$$

where RH is the leaf-surface RH, C_a is the leaf-surface CO_2 concentration (μmol/mol), A is the net photosynthesis rate (μmol CO_2 m^{-2} s^{-1}), m is the slope parameter (unitless), and g_0 (mol m^{-2} s^{-1}) is the intercept of the regression, representing baseline g_s.

The BBK model (Katul et al., 2010) as Equation (2) is an extended version of the BB model that also accounts for the CO_2 compensation point (Γ^*) of assimilation in the absence of dark respiration.

$$g_s = g_0 + m_1 \times \frac{A \times RH}{C_a - \Gamma*}, \tag{2}$$

where m_1 is the slope parameter, and Γ^* is a function of leaf temperature using the same formula as Leuning (1995), shown in Table S1.

The BBL model (Leuning, 1995) is an alternative way to relate g_s to the environment incorporating an empirical dependence on leaf-to-air vapor pressure deficit (D, kPa) as follows:

$$g_s = g_0 + a_1 \times \frac{A}{(C_a - \Gamma*) \times (1 + D/D_0)}, \tag{3}$$

where a_1 is the slope parameter and D_0 is a fitted parameter. A practical issue with Equation (3) is that the parameters a_1 and D_0 are highly correlated (Medlyn, Robinson, Clement, & McMutrie, 2005) and thus not statistically valid to interpret values of a_1 across different tree-species when D_0 is fitted simultaneously. To avoid this issue, we employed a two-stage fitting procedure where we initially fitted BBL for the full dataset to derive D_0 (=0.61), and then assigned the same D_0 throughout all tree-species when estimating tree-species-specific a_1.

The USO model as follows is an optimality model developed by Medlyn et al. (2011), with the slope parameter of g_1.

$$g_s = g_0 + 1.6 \times \left(1 + \frac{g_1}{\sqrt{D}}\right) \times \frac{A}{C_a}. \tag{4}$$

Of particular note, in the original derivation of the g_s models shown above, the intercept term g_0 ensures correct g_s response when A approaches zero. The term g_0 is often thought to represent the cuticular g_s, or the conductance with closed stomata. Similar to Lin et al. (2015), we did not fit g_0. First, fitted values of g_0 and the slope parameter tend to be correlated, meaning that the estimated slope parameters can be ill-posed and differences in the slope parameters among datasets cannot be clearly interpreted. Second,

measuring cuticular conductance instead of fitting the parameter is likely a better means to capture g_0. Since we did not measure cuticular conductance, in our data analysis, we assume $g_0 = 0$ for all tree-species.

To evaluate whether inclusion of Ψ_{leaf} as an additional model variable improves predictions of the four g_s models (Equations 1–4), we adapted the equation below from Anderegg et al. (2017):

$$f_{\Psi_{leaf}} = e^{-\left(\frac{-\Psi_{leaf}}{c}\right)^b},\tag{5}$$

where b and c are two tree-species-specific parameters, which describe the Weibull form of the xylem conductivity functions, and hydraulic conductivity = $k_{max} \times f_{\Psi_{leaf}}$, where k_{max} describes the maximum rate of hydraulic conductance in the absence of water stress, that is, $\Psi_{leaf} = 0$ MPa (Sperry et al., 2017).

Taking BBL as an example, the model that incorporates Ψ_{leaf} is shown below:

$$g_s = g_0 + a_1 \times \frac{A}{(C_a \times \Gamma*) \times (1 + D/D)} \times f_{\Psi_{leaf}}.\tag{6}$$

2.4 | Modeling experiments, model fit and drivers of the slope parameter variation

We first evaluated model choice and whether inclusion of Ψ_{leaf} would improve predictions of the four g_s models through the following three tests: (a) we calculated the model residuals (that we defined as the modeled g_s minus observed g_s) for the modeling scenarios without Ψ_{leaf} and quantified the extent to which these model residuals can be explained by measured Ψ_{leaf}; (b) we performed model optimization for each of the four g_s models with (including three parameters: the slope parameter, b and c) and without (that has just one parameter: the slope parameter) Ψ_{leaf}, and evaluated the model selection with the coefficient of determination (R^2), the root-mean-squared error (RMSE) of the model and the Akaike information criterion (AIC). AIC allows for the determination of relative statistical model robustness and parsimony by estimating the degree to which the inclusion of additional parameters between models improves model fit versus the loss of statistical power; and (c) performed a second model optimization at the tree-species level, but instead of using the optimized Weibull parameters (b and c; Equation 5) for describing the xylem conductivity function as in the second test, we used the tree-species-specific Weibull parameters derived from laboratory-measured stem hydraulic vulnerability curves (Table 1). The model selection was then evaluated through corresponding R^2, RMSE, and AIC.

In addition to the tests including Ψ_{leaf}, we also evaluated the models in their original forms (Equations 1–4). For each g_s model we examined how the abiotic (i.e. site: PNM and SLZ; month-of-measurement: February, March, April and May) and biotic (i.e. tree-species, $n = 15$) factors separately and jointly influence the estimation of the slope parameter used to predict g_s. We started with the scenario that only accounts for the fixed effect, that is, assuming a

common slope parameter for the full dataset. We then performed the analysis iteratively by adding one level of the random effects (i.e. allowing for variation in the slope parameter associated with different abiotic and/or biotic factors) in each analytical scenario, following the order of random effects induced by month, site-month interaction, tree-species and tree-species-month interaction, respectively, until the full random effects were represented in the final analysis. Three metrics (R^2, RMSE and AIC) were also calculated to compare different analytical scenarios.

Additionally, we bootstrapped the full dataset 1,000 times for cross-model performance comparisons. For each bootstrap, we randomly selected 70% of the data to fit parameters and used the remaining 30% for validation. For the validation results (quantified using both the R^2 and RMSE statistics calculated for each iteration), statistical differences between model pairs were identified with t tests.

Last, we derived tree-species-specific slope parameters for each of the four g_s models in their original forms using the ordinary least squared nonlinear model fit. We assessed these slope parameter correlations with all six available plant traits, which have previously been linked with either plant photosynthesis or transpiration. These six plant traits included wood density, LMA, $V_{c,max25}$, LWC, degree of isohydry and pre-dawn Ψ_{leaf}.

3 | RESULTS

3.1 | g_s model performance with and without Ψ_{leaf} as an additional model variable

Regardless of the g_s model chosen, our results showed that adding Ψ_{leaf} as an additional model predictor variable did not appreciably improve model predictions of g_s across all three of our tests of inclusion, that is, (a) examining the relationships between the model residuals of g_s resulting from predictions of g_s by the original model formulations (Equations 1–4) and from model formulations that included representation of field measured Ψ_{leaf} (Figure S4), (b) adding in a single pair of statistically optimized additional parameters (i.e. Weibull parameters b and c; Equation 5) to describe xylem conductivity response to Ψ_{leaf} (Figure 3), and (c) adding in tree-species-specific Weibull parameters derived from laboratory-measured stem hydraulic vulnerability curves (Table 1) to describe xylem conductivity response to Ψ_{leaf} (Figure 4; Figure S5). As shown in Figure S4, we found that the model residuals showed no or very weak relationships ($R^2 = 0.00$–0.04) with Ψ_{leaf} across all the four g_s models analyzed here. This thus provides direct evidence that accounting for the variability in Ψ_{leaf} did not appreciably improve model predictions of g_s for these tropical trees.

When using the optimized tree-species-specific Weibull parameters (Figure 3), we found the optimization results for the model formulations that include Ψ_{leaf} have very similar predictive power (in terms of R^2 and RMSE) compared with the corresponding cases without Ψ_{leaf}, while AIC values indicated that the inclusion of Ψ_{leaf} did not significantly improve model fit and instead reduced model parsimony. This is especially apparent for the scenario of "tree-species-month
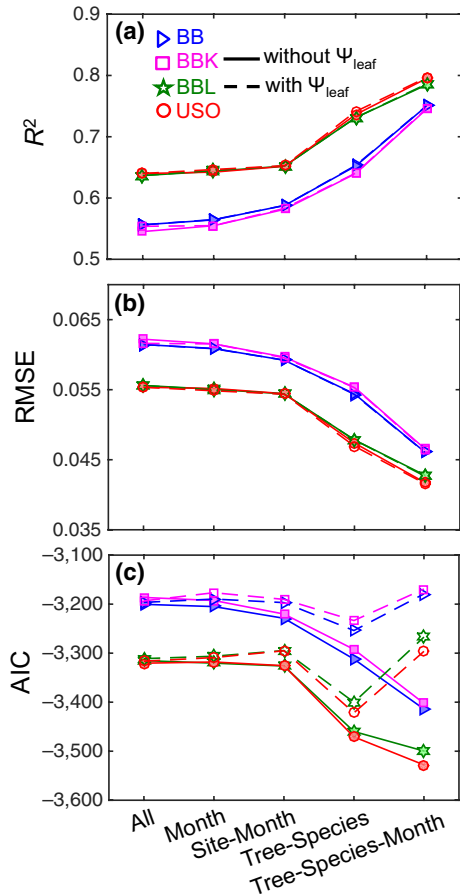
FIGURE 3 Model performance comparisons across different g_s models and with/without including leaf water potential (Ψ_{leaf}). Statistics for the four g_s models (color symbols) that exclude (solid lines) or include (dash lines) Ψ_{leaf} as an additional model predictor variable, including (a) the coefficient of determination (R^2), (b) root-mean-square-error (RMSE) between modeled and observed g_s, and (c) Akaike information criterion (AIC), for the entire dataset (n = 574 observations from 15 tree tree-species). The x-axis represents different scenarios for model treatments of the whole dataset, by separating them according to different combinations among month, site and tree-species. The results shown here are based on the statistically optimized nonlinear model fitting. AIC is a statistic metric that allows inference on the relative quality of statistical models, and the models with relatively lower AIC values are generally chosen over another. The four g_s models are Ball–Berry (BB), Ball–Berry–Katul (BBK), Ball–Berry–Leuning (BBL), and Unified Stomatal Optimization (USO)
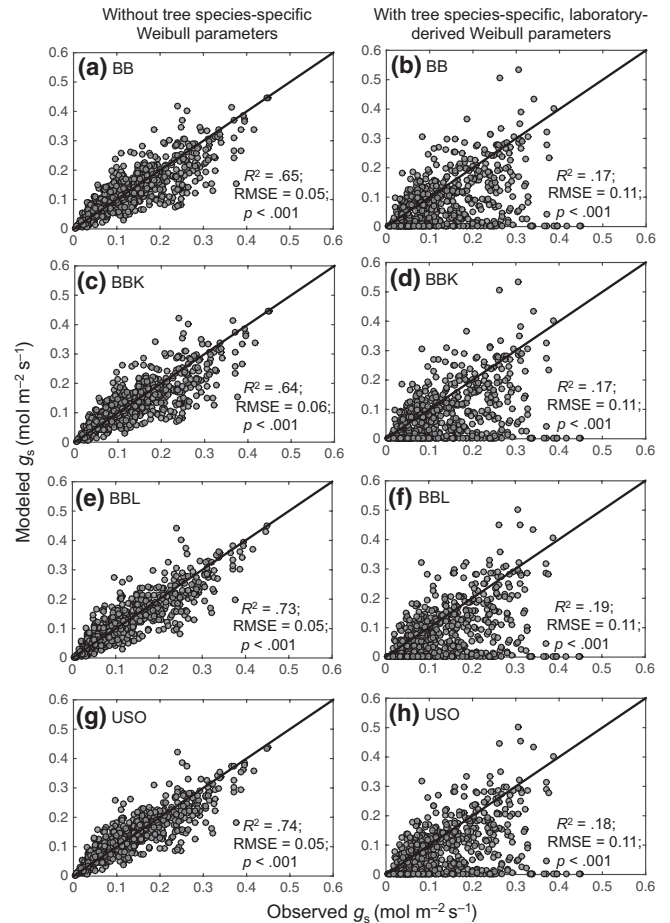
FIGURE 4 Model performance comparisons across g_s models with and without tree-species-specific Weibull parameters. The tree-species-specific Weibull parameters were derived from laboratory-measured stem hydraulic vulnerability response curves (parameters are shown in Table 1) and field measurements of leaf water potential (Ψ_{leaf}). The left hand panels (a, c, e, g) show the results from the four models in their original forms (see Equations 1–4), and the right panels (b, d, f, h) show those same models with formulations that include Ψ_{leaf} and derived Weibull parameters. The four g_s models are Ball–Berry (BB), Ball–Berry–Katul (BBK), Ball–Berry–Leuning (BBL), and Unified Stomatal Optimization (USO). The model results shown here are based on the entire dataset (n = 574 observations from 15 tree-species); tree-species-specific model evaluation is reported in Figure S5 and Table S2. R^2 for coefficient of determination, RMSE for root-mean-square-error, and p for significance level of modeled versus observed g_s correlations. Black lines indicate the 1:1 relationships

interaction" (Figure 3c). For each of the four g_s models the AIC value when including Ψ_{leaf} is far higher than the corresponding case without Ψ_{leaf}, and is also even higher than the scenario of "all" (Figure 3c; which assumes a common slope parameter for the full dataset), indicating that the models with Ψ_{leaf} were over parameterized.

When using the derived tree-species-specific Weibull parameters (as in Table 1) rather than optimized parameters, we found that the performance of g_s models coupled with Ψ_{leaf} was markedly lower than the corresponding cases without Ψ_{leaf} (Figure 4; Figure S5; Table S2). Particularly, at the tree-species level, regardless of the g_s

model chosen, the former cases (with Ψ_{leaf}) only have the predictive power of R^2 = 0.17–0.19 across all 15 tree-species (Figure 4b,d,f,h), while the later cases (without Ψ_{leaf}) have much better model performance (R^2 = 0.64–0.74; Figure 4a,c,e,g).

3.2 | RH-type versus VPD-type g_s models

We now focused on the original g_s models, without further consideration of the addition of a leaf water potential formulation (i.e. Equation 5). When using a common, model specific, slope parameter for the full

dataset, the g_s models captured 56% (BB), 55% (BBK), 64% (BBL) and 65% (USO) of the variability in field-measured g_s (Figure 3). Notably, the two D-type models (BBL and USO), which represent the g_s response to vapor pressure deficit, outperformed the other two RH-type models (BB and BBK), which represent the g_s response to RH. Our bootstrapping analysis and associated t tests also suggested the D-type models had significantly higher model performance compared to the RH-type models (Figure S6; Table S3), with the relative rank among these four models as follows: USO > BBL >> BB > BBK.

3.3 | Abiotic versus biotic control on the stomatal slope parameter

We examined the relative impacts of biotic (i.e. tree-species) and abiotic (i.e. month, site-month interaction) drivers of variation of the slope parameters used in the four g_s models on the ability to predict g_s. For all four models, we observed that accounting for tree-species-specific and tree-species-month-specific variation in the slope parameter provided the most significant improvement in the prediction of field-observed g_s, with a >10% increase in R^2 and ~20% decrease in RMSE% (Figure 3), relative to a common, model specific, slope parameter for the full dataset. In contrast, accounting for month-specific variation in the slope parameter did not improve g_s prediction (Figure 3). In addition, our results showed that accounting for site-month-specific variation in the slope parameter improved g_s prediction only for the two RH-type models but not for the two D-type models. In addition, our results also showed that the two RH-type models had similar model performance, but consistently yielded lower R^2 and higher RMSE than the two D-type models (Figure 3).

3.4 | Large inter-tree-specific variation in slope parameters and their relationships with plant traits

Given the role of tree-species in driving stomatal slope variation (Figure 3), we further explored the potential for important relationships between stomatal slope and tree-species-specific plant traits. To do this we first examined inter-tree-specific variation in the slope parameters and then assessed their correlations with six field-collected plant traits. We found large inter-tree-specific variation in the slope parameters (Figure 5; Figures S7–S9; Table 2), with around two to three fold variation depending on the model choice. Such high inter-tree-specific variation in the slope parameter was also found within each of the two tropical forests, with seven-tree-species average slope parameters and standard deviations of 7.38 ± 1.12 (BB), 6.34 ± 0.95 (BBK), 12.65 ± 2.18 (BBL), and 2.68 ± 0.59 (USO) for PNM, and eight-tree-species average slope parameters and standard deviations of 6.64 ± 1.55 (BB), 5.78 ± 1.35 (BBK), 10.72 ± 2.40 (BBL), and 2.17 ± 0.70 (USO) for SLZ. Similarly, we also observed relatively high inter-tree-specific variation in our plant traits (see Table 1 and Figure 5), including wood density ranging from 0.34 to 0.75 g/m³, LMA (84–154 g/m²), $V_{c,max25}$ (18–85 μmol m⁻² s⁻¹), LWC (46%–65%), degree of isohydry (−0.21 to 1.96; unitless) and pre-dawn Ψ_{leaf} (−1.9 to −0.8 MPa). Exploring the relationship between derived tree-species-specific slope
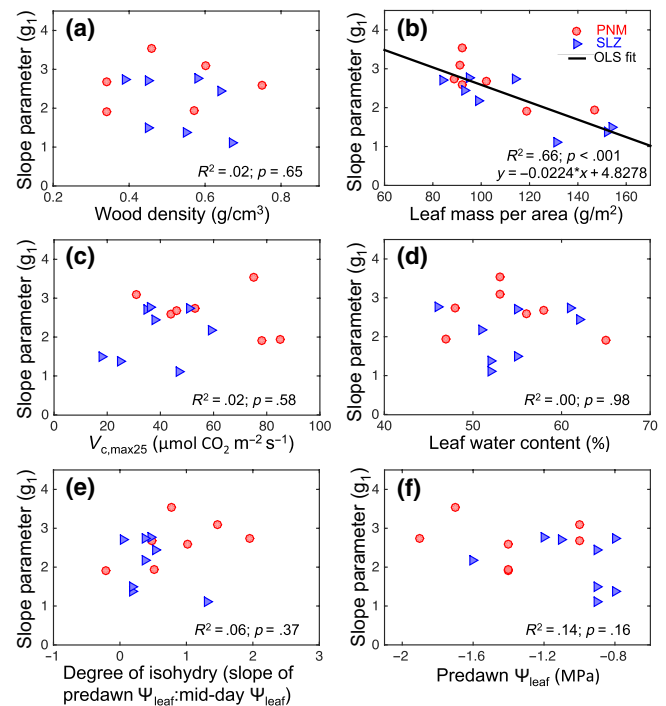

FIGURE 5 Correlations between the tree-species-specific slope parameter (g_1; using the unified stomatal optimization model; Medlyn et al., 2011) and associated plant traits, including (a) wood density, (b) leaf mass per area, (c) $V_{c,max25}$, (d) leaf water content, (e) degree of isohydry (approximated by the slope between predawn and mid-day leaf water potential; Martinez-Vilalta et al., 2014), and (f) predawn leaf water potential (Ψ_{leaf}). Points show tree-species means from the Parque Natural Metropolitano (dry) site (n = 7 tree-species, circles), and the SLZ site (n = 8 tree-species, triangles). R^2 for coefficient of determination, and p for significance level of slope parameter-trait correlation. Fitted lines (ordinary least square regression, OLS) were only shown for significant relationships. Similar results were found for the Ball–Berry model (Figure S7), the Ball–Berry–Katul model (Figure S8), and the Ball–Berry–Leuning model (Figure S9)

parameters and plant traits (Figure 5; Figures S7–S9) yielded only one significant correlation, LMA (R^2 = 0.66–0.67), consistent among all four g_s models. The other five traits we examined, that is, a wood trait (wood density), a leaf photosynthetic trait ($V_{c,max25}$), and three hydraulic traits (LWC, degree of isohydry and pre-dawn Ψ_{leaf}), showed no significant relationships with the slope parameters.

4 | DISCUSSION

Understanding abiotic and biotic controls of g_s and exploring accurate representation of g_s in TBMs has been a core focus in ecology of climate regulation and plant physiology ecology. Here, we used data from two contrasting tropical forests that spanned a large range of environmental conditions associated with diurnal and seasonal variation. We demonstrated that in tropical forests, including Ψ_{leaf} in model formulations did not improve predictions of g_s, and

TABLE 2 Tree-species-specific model optimization results for all four g_s models (i.e. BB, BBK, BBL and USO) using the ordinary least squares nonlinear model fit

Site	Species name	Number of observations	BB			BBK			BBL			USO		
			Slope (m)	R^2	RMSE	Slope (m_1)	R^2	RMSE	Slope (a_1)	R^2	RMSE	Slope (g_1)	R^2	RMSE
PNM	*Albizia adinocephala*	36	7.92 ± 0.09	0.42	0.07	6.82 ± 0.08	0.39	0.07	12.91 ± 0.10	0.60	0.06	2.78 ± 0.03	0.60	0.06
PNM	*Pittoniotis trichantha*	35	8.58 ± 0.10	0.53	0.06	7.38 ± 0.09	0.52	0.07	14.33 ± 0.17	0.57	0.06	3.14 ± 0.04	0.60	0.06
PNM	*Calycophyllum candidissimum*	35	7.00 ± 0.15	0.12	0.06	6.00 ± 0.14	0.11	0.06	12.58 ± 0.20	0.37	0.05	2.61 ± 0.06	0.30	0.05
PNM	*Castilla elastica*	23	7.20 ± 0.16	0.57	0.06	6.19 ± 0.14	0.56	0.06	12.63 ± 0.24	0.76	0.05	2.72 ± 0.07	0.73	0.05
PNM	*Cordia alliodora*	35	8.85 ± 0.21	0.30	0.07	7.55 ± 0.19	0.28	0.07	16.08 ± 0.24	0.53	0.05	3.58 ± 0.07	0.50	0.05
PNM	*Ficus insipida*	35	6.13 ± 0.08	0.60	0.06	5.31 ± 0.07	0.59	0.06	9.88 ± 0.12	0.70	0.05	1.95 ± 0.03	0.68	0.06
PNM	*Luehea seemannii*	32	5.98 ± 0.04	0.74	0.04	5.12 ± 0.03	0.74	0.04	10.17 ± 0.07	0.66	0.05	1.96 ± 0.02	0.77	0.04
SLZ	*Carapa guianensis*	41	5.01 ± 0.06	0.56	0.03	4.38 ± 0.06	0.55	0.03	8.18 ± 0.10	0.65	0.03	1.44 ± 0.03	0.63	0.03
SLZ	*Guatteria dumetorum*	44	7.90 ± 0.06	0.34	0.05	6.88 ± 0.05	0.32	0.06	13.00 ± 0.09	0.50	0.05	2.80 ± 0.02	0.48	0.05
SLZ	*Miconia borealis*	41	6.79 ± 0.06	0.47	0.06	5.91 ± 0.05	0.47	0.06	11.20 ± 0.10	0.55	0.06	2.28 ± 0.03	0.53	0.06
SLZ	*Tachigali versicolor*	45	8.30 ± 0.08	0.44	0.06	7.25 ± 0.07	0.43	0.06	13.03 ± 0.12	0.53	0.05	2.85 ± 0.03	0.51	0.06
SLZ	*Terminalia amazonia*	45	4.43 ± 0.03	0.73	0.02	3.86 ± 0.03	0.72	0.02	7.31 ± 0.04	0.77	0.02	1.14 ± 0.01	0.76	0.02
SLZ	*Tocoyena pittieri*	44	7.19 ± 0.08	0.56	0.06	6.26 ± 0.07	0.55	0.06	11.92 ± 0.14	0.60	0.06	2.48 ± 0.04	0.62	0.05
SLZ	*Virola multiflora*	43	5.23 ± 0.07	0.52	0.04	4.55 ± 0.06	0.51	0.04	8.32 ± 0.11	0.62	0.03	1.53 ± 0.03	0.59	0.03
SLZ	*Vochysia ferruginea*	46	8.26 ± 0.05	0.56	0.07	7.18 ± 0.04	0.55	0.07	12.80 ± 0.08	0.62	0.06	2.83 ± 0.02	0.62	0.06

Note: The model results shown below including the two statistic metrics for model performance (R^2 and RMSE) and the best fitted stomatal slope (mean ± standard deviation). The four g_s models are BB, BBK, BBL, and USO, and the two crane sites in Panama include the PNM site, and the SLZ site.

Abbreviations: BB, Ball–Berry; BBK, Ball–Berry–Katul; BBL, Ball–Berry–Leuning; PNM, Parque Natural Metropolitano; RMSE, root-mean-squared error; SLZ, San Lorenzo; USO, Unified Stomatal Optimization.

the models that represent g_s response to vapor pressure deficit (i.e. D-type models, BBL and USO) performed better than the models based on RH (i.e. RH-type models, BB and BBK). Additionally, we demonstrated that accounting for the variation in the slope parameters across tree-species significantly improved model estimates of g_s, while accounting for the variation in the slope parameters induced by abiotic factors (i.e. month and site-month interaction) did not appreciably improve model performance. Finally, we explored potential relationships between the slope parameters and six plant traits that correlate with photosynthesis or transpiration, and identified only one leaf trait, LMA, that had a significant correlation with the slope parameter derived from each of the four g_s model formulations.

4.1 | Modeling g_s with or without Ψ_{leaf}

Several recent studies have suggested that Ψ_{leaf} should be incorporated into models of g_s (e.g. Anderegg et al., 2017; Drake et al., 2017; Sperry et al., 2017; Venturas et al., 2018; Zhou et al., 2014). However, in our study the data do not support this argument, at least for the tropical evergreen canopy trees analyzed here (Figures 3 and 4; Figure S5). This result, while in contrast with previous work, is not unexpected. For example, in a recent synthesis study, Anderegg et al. (2017) used a dataset of 24 woody plant species spanning global forest biomes to examine the effect of Ψ_{leaf} on model prediction of g_s. Their results showed that for the majority of tree species analyzed, inclusion of Ψ_{leaf} did not significantly improve prediction of g_s, which is consistent with what we found here. Meanwhile, they did find that for four tree-species g_s prediction was significantly improved with Ψ_{leaf} (i.e. Δ-AIC > 3 with increase in R^2 by 10% or more). We note that those four tree-species were derived from studies that examined drought impacts on a water-limited glasshouse plant (Arango-Velez, Zwiazek, Thomas, & Tyree, 2011), saplings (Wolfe et al., 2016), and two woody plants (including an evergreen tree in an Australian tropical dry forest, and a juniper tree in northern Arizona pinyon-juniper woodland) without explicitly accounting for the interactive effect of both leaf phenology and seasonal variability in soil moisture content (Choat, Ball, Luly, Donnelly, & Holtum, 2006; Koepke & Kolb, 2012).

Since our analysis focused on evergreen tropical canopy trees that experience seasonal variability in soil moisture content (Figure 2), we hypothesize that there are two major reasons for the discrepancy between previous results and those of this study. First, including Ψ_{leaf} in g_s formulations might be more important for water-limited plants (Arango-Velez et al., 2011; Venturas et al., 2018; Zhou et al., 2014), for example, saplings or glasshouse plants, but might not improve model predictions for mature trees. This is especially relevant for evergreen tropical trees that can maintain green leaves year-round, and have deep and extensive root systems that enable access to moist soil during seasonal droughts (Giardina et al., 2018; Guan et al., 2015; Meinzer et al., 1999; Nepstad et al., 1994). Therefore, conclusions drawn from glasshouse plants

or saplings should be used with caution when considering natural forest ecosystems, particularly tropical forests. Second, the slope parameters in the original g_s models (i.e. Equations 1–4) likely vary with leaf age (e.g. Albert et al., 2018), which covaries with Ψ_{leaf} (and many other traits) over the season in seasonal forests (e.g. Koepke & Kolb, 2012; Xu & Baldocchi, 2003), but not in evergreen forests where mixed leaf ages are often found year round (e.g. Lopes et al., 2016; Wu et al., 2016). Thus, including Ψ_{leaf} can improve predictions of g_s seasonality over leaves of different ages, but may not be a significant factor when controlling for leaf age as this study. This hypothesis is consistent with several studies (e.g. Albert et al., 2018; Jordan, Brown, & Thomas, 1975; Pantin et al., 2012; Rogers et al., 2012) that show a strong age-dependence of leaf g_s under controlled environmental conditions. However, additional field and manipulation studies are needed to fully elucidate the mechanisms and scales at which leaf properties, such as Ψ_{leaf}, may regulate g_s in addition to other, potentially correlated leaf properties.

There was still a weak but significant relationship between Ψ_{leaf} and the g_s residuals in three of the four g_s models in their original forms (Figure S4). Higher residuals at lower Ψ_{leaf} indicate that the models tended to overestimate g_s at low Ψ_{leaf} and suggest that there is indeed room to improve the models by incorporating Ψ_{leaf}. However, the proposed model improvements with Ψ_{leaf} (i.e. Anderegg et al., 2017) that we tested failed to improve model performance (Figures 3 and 4; Figure S5; Table S2). We identified three potential reasons. First, it is likely true that Ψ_{leaf} can help regulate g_s variation, particularly when leaf or soil water potential is below certain thresholds (e.g. under severe droughts or when Ψ_{leaf} is close to leaf turgor loss point; Brodribb & Holbrook, 2003; Rodriguez-Dominguez et al., 2016; Venturas et al., 2018), but not within the range of variability we witnessed. As such, Ψ_{leaf} does not play a large role in regulating the range of observed g_s values in this study (Figure 3; Figure S4). Second, the additional parameters (i.e. Weibull parameters of b and c as shown in Equation 5) required to fit the model come with their own uncertainties, since they are based on the laboratory-measured hydraulic conductivity responses (e.g. Wolfe et al., 2016). Such uncertainty can propagate into the fitting scheme leading to a lower model performance as observed in Figure 4 and Figure S5. Lastly, the water potential in the leaves can be more negative than the water potential in the stem xylem, and this should be taken into account when using Ψ_{leaf} to parameterize stem vulnerability curves within g_s models. For example, as in Figure S5, the stem hydraulic vulnerability curves suggest that most of trees we studied would close their stomata (i.e. $f_{\Psi_{leaf}} = 0$) when Ψ_{leaf} is lower than −2MPa, while field observations showed that the stomata were still open and that leaves were photosynthesizing, even when Ψ_{leaf} < −2MPa. The difference in water potential between leaf and stem is quite difficult to quantify in nature, as it varies largely with tree-species, growth environment and plant traits (Christoffersen et al., 2016; Nolf et al., 2015). For example, in tropical plants, water storage and plant atmospheric water absorption have been shown to be effective in buffering diurnal fluctuation of xylem water potential (Bartlett, Detto, & Pacala, 2019; Binks et al., 2019; Meinzer, James, Goldstein, & Woodruff, 2003).

Thus, including Ψ_{leaf} in the g_s models should be done by considering a more comprehensive quantification of the entire soil-plant-atmosphere continuum (e.g. Giardina et al., 2018).

Regardless of the above-mentioned limitations, plant hydraulics models (e.g. Sperry et al., 2017; Wolf, Anderegg, & Pacala, 2016) that rely on stem xylem conductivity response functions (as Equation 5) can still provide a useful framework for theoretical simulation or deduction of plant optimal response to soil and atmospheric water stress. However, the uncertainty associated with the Weibull parameters (based on direct measurements of hydraulic conductivity), the fact that the optimal theory of stomata control might operate at a longer timescale (e.g. Buckley, Sack, & Farquhar, 2017; Lin et al., 2018), rather than at the instantaneous timescale as explored here, as well as that the exact biological mechanisms that contribute to the hydraulic cost (e.g. damage, repair or loss of opportunity) underlying the optimality theory have not yet been identified or readily measured, further suggests that more research is needed to determine the most appropriate means of incorporating such optimal plant hydraulics theory into process-based g_s models that are integrated into TBMs.

4.2 | Stomatal model choice: *D*-type versus RH-type g_s models

Although *D*-type models have been increasingly advocated by plant physiologists (e.g. Medlyn et al., 2011; Rogers, Medlyn, et al., 2017), both *D*-type versus RH-type models are still widely used in many TBMs (e.g. Franks et al., 2018; Knauer et al., 2017). Meanwhile, in-situ gas exchange measurements from mature tall trees to examine the difference across these two model types are rare. Furthermore, in moist tropical forests, seasonal variation in air temperature is small (e.g. Figure S2b), and consequently *D* and RH are typically more correlated than in other biomes; therefore, we expected only minor differences in performance between *D*- and RH-type models in the tropics. To evaluate the correlation between RH- and *D*-type models, we made measurements over full diurnal cycles and a dry season in a particularly dry El Niño year (Figure 2), which captured a wide range of natural variability in RH and *D* experienced in these forests. The two *D*-type models significantly outperformed the two RH-type models both across and within our dataset (*n* = 15 tree-species; Figure 3; Table 2), suggesting that *D*-type models should be used for modeling carbon and water fluxes in tropical forest ecosystems, and potentially, also in many other ecosystems, particularly those where *D* and RH are not tightly correlated, for example, savanna. The cross-model comparisons between BB (which accounts for the RH effect) and BBK (which accounts for RH and includes CO_2 compensation point, Γ^*), shows that including Γ^* did not improve model performance (Figure 3). Therefore, the improved performance of BBL (which accounts for *D* and Γ^* effects) relative to BB was primarily because BBL captures g_s response to *D*, consistent with the concept that stomata respond directly to *D* rather than to RH (Aphalo & Jarvis, 1991; Eamus et al., 2008).

Our results also show that the two *D*-type models generated comparable model performance for our dataset, with USO yielding a small but significantly better model performance than BBL (Figure 3; Figure S6; Table S3). This finding is consistent with several recent studies both relying on empirical observations (e.g. Medlyn et al., 2011) and mathematical simulations of optimal stomatal behavior (e.g. Wolf et al., 2016) for a range of environmental conditions (e.g. C_a within the range of 375–425 ppm). However, as Wolf et al. (2016) point out, due to the fundamental difference in the forms of *D* response in BBL ($\sim D^{-1}$) and USO ($\sim D^{-1/2}$), the predictions of BBL and USO models will differ when C_a exceeds 425 ppm, which is expected to occur in the next one to two decades. Therefore, we advocate that USO should be favored for modeling g_s response to *D*, particularly in TBMs that aim to capture the impact of global change on the climate system.

4.3 | Variation in the slope parameter, sources of variability, and its impact on g_s modeling

We observed large variation in the slope parameter across the sampled 15 tree-species. Such biotic slope parameter variation (e.g. g_1 used in USO varied from 1.14 to 3.58) is present at both sites (Figure 5; Table 2), and corresponds roughly to the range assigned to six of 10 global PFTs in a recent synthesis using the USO approach (Lin et al., 2015). In particular, our observed g_1 range encompasses the g_1 value of 1.84 for a tropical tree in Caxiuana National Forest Reserve in the eastern Amazon (Lin et al., 2015), overlaps extensively with the g_1 (3.00–3.79) for three tropical tree-species in Australia (Lin et al., 2015), and is within the range of g_1 (0.9–6.2) for 21 tree-species surveyed in central tropical Africa (Hasper et al., 2017), including canopy and understory trees. Such agreement with previous findings suggests that our results could be broadly applicable to other forests in the tropics. Additionally, we observed that our g_1 range is largely lower than an average g_1 of 4.23 across a set of tree species sampled in a tropical forest in French Guiana. This might be attributable to the inconsistent approach used for g_1 estimate, for example, only one g_1 value was estimated for the whole dataset due to insufficient replication (Lin et al., 2015). In the analysis presented by Lin et al. (2015) they estimated a g_1 of 3.77 for a generic tropical rainforest PFT, which is higher than our observed g_1 range (1.14–3.58). However, this mean g_1 included the high estimate from French Guiana. When excluding the French Guiana data-point, the mean g_1 estimate based on Lin et al. (2015) is 3.02, which is well within our g_1 range. The particularly lower g_1 values (i.e. all lower than 3.77 and 13/15 tree-species lower than 3.02) observed in our study could also reflect an acclimation to interannual climate variability (e.g. Reyer et al., 2013), for example, the drier El Niño year experienced in our study, which started at the end of 2014, peaked in late 2015, and ended in May 2016 (Liu et al., 2017). The increasing atmospheric water deficit in the drought year could push plants to evolve a more conservative strategy in order to cope with increasing hydrological stress with El Niño droughts (Cowan & Farquhar, 1977). Clearly there is a need

for a deeper understanding of variation in g_1 in tropical forests, of particularly value would be replicated measurements that span variation in soil fertility, climate, canopy structure, and leaf phenology and morphology.

With the observed large inter-tree-specific variation in slope parameter, we further showed that accounting for such biotic variation led to improved model estimates of g_s (Figure 3). This finding is consistent with previous work, which illustrated the diversity in stomatal slope is integral to modelling plant water fluxes (Wolz et al., 2017). Our results did not show that accounting for the abiotic (e.g. month, site-month interaction) effects of slope parameter variation improved D-type g_s modeling (Figure 3). However, we observed that variation in the slope parameter induced by the tree-species-month interaction was the second most important factor for improving g_s modeling of the full dataset. This may reflect differential drought-induced acclimation of the slope parameter across tree-species as reported previously (e.g. Heroult et al., 2013; Zhou, Medlyn, & Prentice, 2015). Furthermore, we controlled for leaf age in our experimental design but it is clear that accounting for potential phenological variation in the slope parameter at the longer timescale will be critical to more accurately represent the seasonal variation in canopy fluxes and the modeling of g_s under natural conditions (Albert et al., 2018) and warrants further exploration.

We did not find that month-associated (i.e. month-specific and site-month-specific) slope parameter variation was important for g_s modeling, particularly for D-type models. This suggests that D-type g_s models are able to accurately represent g_s response to seasonal environmental variability. Further extension of our leaf-level findings to interpret ecosystem-scale transpiration seasonality would require the understanding of leaf phenology and forest composition, in particular how the slope parameter varies with different phenophases, including leaf age (as discussed above) and leaf habits (evergreen vs. deciduous trees; Bohlman, 2010), as well as the seasonal and interannual variation in these phenophases (e.g. Detteo, Wright, Calderón, & Muller-Landau, 2018; Lopes et al., 2016; Wu et al., 2018).

4.4 | Plant trait relationships with the inter-tree-specific slope parameter

Our results show that LMA was highly correlated with the inter-tree-specific slope parameter for all four g_s models (Figure 5; Figures S7–S9). The five other traits we investigated showed weak or no correlation with the slope parameter. Wood density has recently been shown to have a significant relationship with the slope parameter at the global scale (Lin et al., 2015), but was not significantly correlated with the slope parameter in this study. It is possible that over a narrower geographic range with less variability in wood density (the range of wood density is 0.34–0.75 in this study vs. 0.35–1.1 in Lin et al., 2015) the relationship may not hold. We hypothesized that $V_{c,max25}$ may have a negative relationship with the slope parameter because as the slope parameter decreases, water use efficiency rises and the effective C_i/C_a in a low slope parameter tree-species (with

a lower g_s for a given A) might require a higher $V_{c,max25}$ in order to maintain the same A compared with plant with a larger value of the slope parameter. The lack of a relationship may imply that it will be important to consider the role of mesophyll conductance, especially for model applications (Sun et al., 2014). We also anticipated that measurements of leaf hydrological traits, that is, leaf water content, degree of isohydry and pre-dawn Ψ_{leaf}, may have correlations with the slope parameter, given the link between these parameters and model formulations that include hydraulic limitations (e.g. Rogers, Medlyn, et al., 2017; Tuzet, Perrier, & Luening, 2003; Williams et al., 1996). The lack of a correlation in this study suggests that Ψ_{leaf}, which changes markedly during the day, may not share a clear mechanistic link to the slope parameter, which likely acclimates to the environment over much longer timescales.

The underlying reason for the observed slope parameter–LMA relationship might be that LMA is subject to hydrological constraints (Cavaleri, Oberbauer, Clark, Clark, & Ryan, 2010), and results from a long-term evolutionary tradeoff between carbon gain and water loss (Terashima, Miyazawa, & Hanba, 2001). As such, thicker leaves (with higher LMA) are more resistant to water loss, resulting in a higher intrinsic water use efficiency (and a lower slope parameter; Figure 1). Consequently, a negative slope parameter–LMA relationship was observed in this study. Likewise, higher LMA enables leaf temperature to remain nearer to the photosynthetic optimum under conditions of varying air temperature (Michaletz et al., 2015, 2016), again maximizing water use efficiency and promoting a negative slope parameter–LMA relationship. Furthermore, leaves with higher LMA generally have lower mesophyll conductance (Niinemets, Díaz-Espejo, Flexas, Galmés, & Warren, 2009), which could increase photosynthesis without excessive water cost. Consequently, photosynthesis of high LMA tree-species might be less sensitive to stomatal conductance, resulting in a lower slope parameter value. Although these previous studies provide some explanation of the observed slope parameter–LMA relationship, elucidation of the mechanism underlying this relationship is still required. In addition, the LMA–slope parameter relationship presented in this study is based on upper canopy leaf samples of only 15 evergreen canopy tree-species. Therefore, whether the relationship can be extended to broader scenarios, for example, across vertical canopy profiles, different tropical forests, variation in leaf age and soil moisture content, is pending further examination.

The finding that LMA correlates with the slope parameter is encouraging, as LMA is an easy-to-measure leaf trait that is widely used in the plant ecology community and well represented in plant trait databases; for example, the TRY database has LMA entries for over 10,000 species (Díaz et al., 2016). Our observation suggests that it might be possible for next generation TBMs to implement trait-based parameterization of the slope parameter following the approach used for other trait-based modeling components (e.g. photosynthesis, phenology and plant hydraulics) already explored in TBMs (e.g. Fisher et al., 2015; Franks et al., 2018; Xu et al., 2016) and thereby improve representation of carbon and water dynamics in tropical ecosystems.

Additionally, recent work on spectroscopic remote sensing suggests that it is feasible to remotely estimate LMA at the leaf and canopy scales (Asner et al., 2011; Serbin, Singh, McNeil, Kingdon, & Townsend, 2014; Singh, Serbin, McNeil, Kingdon, & Townsend, 2015), and as such, if this LMA–stomatal slope relationship holds it may be possible to derive large-scale estimates of the slope parameter across space and time using the suite of current and planned remote sensing systems (Stavros et al., 2017).

ACKNOWLEDGEMENTS

AUTHOR CONTRIBUTIONS

J.W., S.P.S., B.T.W., and A.R. designed the research. All authors contributed to data collection. J.W., S.P.S., K.S.E., B.T.W., M.D., S.J.W. and A.R. performed the data analysis. J.W. drafted the paper and all authors contributed to writing of the manuscript.

ORCID

Jin Wu https://orcid.org/0000-0001-8991-3970

Shawn P. Serbin https://orcid.org/0000-0003-4136-8971

Kim S. Ely https://orcid.org/0000-0002-3915-001X

Brett T. Wolfe https://orcid.org/0000-0001-7535-045X

L. Turin Dickman https://orcid.org/0000-0003-3876-7058

Charlotte Grossiord https://orcid.org/0000-0002-9113-3671

Sean T. Michaletz https://orcid.org/0000-0003-2158-6525

Adam D. Collins https://orcid.org/0000-0001-9554-5190

Nate G. McDowell https://orcid.org/0000-0002-2178-2254

Alistair Rogers https://orcid.org/0000-0001-9262-7430

REFERENCES

Albert, L. P., Wu, J., Prohaska, N., Camargo, P. B., Huxman, T. E., Tribuzy, E. S., … Saleska, S. R. (2018). Age-dependent leaf function and consequences for crown-scale carbon uptake during the dry season in an Amazon evergreen forest. *New Phytologist*, *219*, 870–884. https://doi.org/10.1111/nph.15056

Anderegg, W. R., Wolf, A., Arango-Velez, A., Choat, B., Chmura, D. J., Jansen, S., … Pacala, S. (2017). Plant water potential improves prediction of empirical stomatal models. *PLoS ONE*, *12*(10), https://doi.org/10.1371/journal.pone.0185481

Aphalo, P. J., & Jarvis, P. G. (1991). Do stomata respond to relative humidity? *Plant, Cell & Environment*, *14*(1), 127–132. https://doi.org/10.1111/j.1365-3040.1991.tb01379.x

Arango-Velez, A., Zwiazek, J. J., Thomas, B. R., & Tyree, M. T. (2011). Stomatal factors and vulnerability of stem xylem to cavitation in poplars. *Physiologia Plantarum*, *143*(2), 154–165. https://doi.org/10.1111/j.1399-3054.2011.01489.x

Asner, G. P., Martin, R. E., Tupayachi, R., Emerson, R., Martinez, P., Sinca, F., … Lugo, A. E. (2011). Taxonomy and remote sensing of leaf mass per area (LMA) in humid tropical forests. *Ecological Applications*, *21*(1), 85–98. https://doi.org/10.1890/09-1999.1

Baldocchi, D., & Meyers, T. (1998). On using eco-physiological, micrometeorological and biogeochemical theory to evaluate carbon dioxide, water vapor and trace gas fluxes over vegetation: A perspective. *Agricultural and Forest Meteorology*, *90*(1–2), 1–25. https://doi.org/10.1016/S0168-1923(97)00072-5

Ball, J. T., Woodrow, I. E., & Berry, J. A. (1987). A model predicting stomatal conductance and its contribution to the control of photosynthesis under different environmental conditions. In J. Biggen (Ed.), *Progress in photosynthesis research* (pp. 221–224). Dordrecht, the Netherlands: Springer.

Bartlett, M. K., Detto, M., & Pacala, S. W. (2019). Predicting shifts in the functional composition of tropical forests under increased drought and CO_2 from trade-offs among plant hydraulic traits. *Ecology Letters*, *22*, 67–77. https://doi.org/10.1111/ele.13168

Bauerle, W. L., Daniels, A. B., & Barnard, D. M. (2014). Carbon and water flux responses to physiology by environment interactions: A sensitivity analysis of variation in climate on photosynthetic and stomatal parameters. *Climate Dynamics*, *42*(9–10), 2539–2554. https://doi.org/10.1007/s00382-013-1894-6

Beer, C., Reichstein, M., Tomelleri, E., Ciais, P., Jung, M., Carvalhais, N., … Papale, D. (2010). Terrestrial gross carbon dioxide uptake: Global distribution and covariation with climate. *Science*, *329*(5993), 834–838. https://doi.org/10.1126/science.1184984

Bernacchi, C. J., Bagley, J. E., Serbin, S. P., Ruiz-Vera, U. M., Rosenthal, D. M., & VanLoocke, A. (2013). Modelling C_3 photosynthesis from the chloroplast to the ecosystem. *Plant, Cell & Environment*, *36*(9), 1641–1657. https://doi.org/10.1111/pce.12118

Bernacchi, C. J., Leakey, A. D., Heady, L. E., Morgan, P. B., Dohleman, F. G., McGrath, J. M., … Ort, D. R. (2006). Hourly and seasonal variation in photosynthesis and stomatal conductance of soybean grown at future CO_2 and ozone concentrations for 3 years under fully open-air field conditions. *Plant, Cell & Environment*, *29*(11), 2077–2090. https://doi.org/10.1111/j.1365-3040.2006.01581.x

Binks, O., Mencuccini, M., Rowland, L., da Costa, A. C., de Carvalho, C. J. R., Bittencourt, P., … Meir, P. (2019). Foliar water uptake in Amazonian trees: Evidence and consequences. *Global Change Biology*, *25*(8), 2678–2690. https://doi.org/10.1111/gcb.14666

Bohlman, S. A. (2010). Landscape patterns and environmental controls of deciduousness in forests of central Panama. *Global Ecology and Biogeography*, *19*(3), 376–385. https://doi.org/10.1111/j.1466-8238.2009.00518.x

Bonan, G. B. (2008). Forests and climate change: Forcings, feedbacks, and the climate benefits of forests. *Science*, *320*(5882), 1444–1449.

Brodribb, T. J., & Holbrook, N. M. (2003). Stomatal closure during leaf dehydration, correlation with other leaf physiological traits. *Plant Physiology*, *132*(4), 2166–2173. https://doi.org/10.1104/pp.103.023879

Buckley, T. N., Sack, L., & Farquhar, G. D. (2017). Optimal plant water economy. *Plant, Cell & Environment*, *40*(6), 881–896. https://doi.org/10.1111/pce.12823

Cavaleri, M. A., Oberbauer, S. F., Clark, D. B., Clark, D. A., & Ryan, M. G. (2010). Height is more important than light in determining leaf morphology in a tropical forest. *Ecology*, *91*(6), 1730–1739. https://doi.org/10.1890/09-1326.1

Choat, B., Ball, M. C., Luly, J. G., Donnelly, C. F., & Holtum, J. A. (2006). Seasonal patterns of leaf gas exchange and water relations in dry rain forest trees of contrasting leaf phenology. *Tree Physiology*, *26*(5), 657–664. https://doi.org/10.1093/treephys/26.5.657

Christoffersen, B. O., Gloor, E., Fauset, S., Fyllas, N. M., Galbraith, D. R., Baker, T. R., ... Meir, P. (2016). Linking hydraulic traits to tropical forest function in a size-structured and trait-driven model (TFS v. 1-Hydro). *Geoscientific Model Development*, 9, 4227–4255. https://doi.org/10.5194/gmd-9-4227-2016

Cowan, I. R., & Farquhar, G. D. (1977). Stomatal function in relation to leaf metabolism and environment. *Symposia of the Society for Experimental Biology*, 31, 471–505.

Detto, M., Wright, S. J., Calderón, O., & Muller-Landau, H. C. (2018). Resource acquisition and reproductive strategies of tropical forest in response to the El Niño-Southern Oscillation. *Nature Communications*, 9(1), 913. https://doi.org/10.1038/s41467-018-03306-9

Díaz, S., Kattge, J., Cornelissen, J. H., Wright, I. J., Lavorel, S., Dray, S., ... Gorné, L. D. (2016). The global spectrum of plant form and function. *Nature*, 529(7585), 167–171.

Dickman, L. T., McDowell, N. G., Grossiord, C., Collins, A. D., Wolfe, B. T., Detto, M., ... Chambers, J. Q. (2019). Homoeostatic maintenance of nonstructural carbohydrates during the 2015–2016 El Niño drought across a tropical forest precipitation gradient. *Plant, Cell & Environment*, 42(5), 1705–1714. https://doi.org/10.1111/pce.13501

Dietze, M. C., Serbin, S. P., Davidson, C., Desai, A. R., Feng, X., Kelly, R., ... Wang, D. (2014). A quantitative assessment of a terrestrial biosphere model's data needs across North American biomes. *Journal of Geophysical Research: Biogeosciences*, 119(3), 286–300. https://doi.org/10.1002/2013JG002392

Drake, J. E., Power, S. A., Duursma, R. A., Medlyn, B. E., Aspinwall, M. J., Choat, B., ... Tissue, D. T. (2017). Stomatal and non-stomatal limitations of photosynthesis for four tree species under drought: A comparison of model formulations. *Agricultural and Forest Meteorology*, 247, 454–466. https://doi.org/10.1016/j.agrformet.2017.08.026

Eamus, D., Taylor, D. T., Macinnis-NG, C. M., Shanahan, S., & de Silva, L. (2008). Comparing model predictions and experimental data for the response of stomatal conductance and guard cell turgor to manipulations of cuticular conductance, leaf-to-air vapour pressure difference and temperature: Feedback mechanisms are able to account for all observations. *Plant, Cell & Environment*, 31(3), 269–277. https://doi.org/10.1111/j.1365-3040.2007.01771.x

Ely, K., Rogers, A., Serbin, S., Wu, J., Wolfe, B., Dickman, T., ... Michaletz, S. (2018a). Leaf mass area, Feb2016-May2016, PA-SLZ, PA-PNM, PA-BCI: Panama. NGEE Tropics Data Collection, https://doi.org/10.15486/ngt/1411973

Ely, K., Rogers, A., Serbin, S., Wu, J., Wolfe, B., Dickman, T., ... Michaletz, S. (2018b). Leaf sample detail, Feb2016-May2016, PA-SLZ, PA-PNM, PA-BCI: Panama. NGEE Tropics Data Collection, https://doi.org/10.15486/ngt/1411971

Fisher, R. A., Muszala, S., Verteinstein, M., Lawrence, P., Xu, C., McDowell, N. G., ... Bonan, G. (2015). Taking off the training wheels: The properties of a dynamic vegetation model without climate envelopes. *Geoscientific Model Development Discussions*, 8(4), 3593–3619. https://doi.org/10.5194/gmd-8-3593-2015

Franks, P. J., Bonan, G. B., Berry, J. A., Lombardozzi, D. L., Holbrook, N. M., Herold, N., & Oleson, K. W. (2018). Comparing optimal and empirical stomatal conductance models for application in Earth system models. *Global Change Biology*, 24, 5708–5723. https://doi.org/10.1111/gcb.14445

Giardina, F., Konings, A. G., Kennedy, D., Alemohammad, S. H., Oliveira, R. S., Uriarte, M., & Gentine, P. (2018). Tall Amazonian forests are less sensitive to precipitation variability. *Nature Geoscience*, 11, 405–409. https://doi.org/10.1038/s41561-018-0133-5

Guan, K., Pan, M., Li, H., Wolf, A., Wu, J., Medvigy, D., ... Lyapustin, A. I. (2015). Photosynthetic seasonality of global tropical forests constrained by hydroclimate. *Nature Geoscience*, 8(4), 284–289. https://doi.org/10.1038/ngeo2382

Hasper, T. B., Dusenge, M. E., Breuer, F., Uwizeye, F. K., Wallin, G., & Uddling, J. (2017). Stomatal CO_2 responsiveness and photosynthetic capacity of tropical woody species in relation to taxonomy and functional traits. *Oecologia*, 184(1), 43–57.

Heroult, A., Lin, Y. S., Bourne, A., Medlyn, B. E., & Ellsworth, D. S. (2013). Optimal stomatal conductance in relation to photosynthesis in climatically contrasting Eucalyptus species under drought. *Plant, Cell & Environment*, 36(2), 262–274.

Jefferson, J. L., Maxwell, R. M., & Constantine, P. G. (2017). Exploring the sensitivity of photosynthesis and stomatal resistance parameters in a land surface model. *Journal of Hydrometeorology*, 18(3), 897–915. https://doi.org/10.1175/JHM-D-16-0053.1

Jordan, W. R., Brown, K. W., & Thomas, J. C. (1975). Leaf age as a determinant in stomatal control of water loss from cotton during water stress. *Plant Physiology*, 56(5), 595–599. https://doi.org/10.1104/pp.56.5.595

Kattge, J., Díaz, S., Lavorel, S., Prentice, I. C., Leadley, P., Bönisch, G., ... Wirth, C. (2011). TRY–a global database of plant traits. *Global Change Biology*, 17(9), 2905–2935. https://doi.org/10.1111/j.1365-2486.2011.02451.x

Katul, G., Manzoni, S., Palmroth, S., & Oren, R. (2010). A stomatal optimization theory to describe the effects of atmospheric CO_2 on leaf photosynthesis and transpiration. *Annals of Botany*, 105(3), 431–442. https://doi.org/10.1093/aob/mcp292

Knauer, J., Zaehle, S., Reichstein, M., Medlyn, B. E., Forkel, M., Hagemann, S., & Werner, C. (2017). The response of ecosystem water-use efficiency to rising atmospheric CO_2 concentrations: Sensitivity and large-scale biogeochemical implications. *New Phytologist*, 213(4), 1654–1666.

Koepke, D. F., & Kolb, T. E. (2012). Species variation in water relations and xylem vulnerability to cavitation at a forest-woodland ecotone. *Forest Science*, 59(5), 524–535. https://doi.org/10.5849/forsci.12-053

Kowalczyk, E. A., Wang, Y. P., Law, R. M., Davies, H. L., McGregor, J. L., & Abramowitz, G. (2006). The CSIRO Atmosphere Biosphere Land Exchange (CABLE) model for use in climate models and as an offline model. *CSIRO Marine and Atmospheric Research Paper 013*. Aspendale, Vic., Australia. Retrieved from http://www.cmar.csiro.au/e-print/open/kowalczykea_2006a.pdf

Lawson, T., & Vialet-Chabrand, S. (2018). Speedy stomata, photosynthesis and plant water use efficiency. *New Phytologist*, 221, 93–98. https://doi.org/10.1111/nph.15330

LeBauer, D., Kooper, R., Mulrooney, P., Rohde, S., Wang, D., Long, S. P., & Dietze, M. C. (2018). BETYdb: A yield, trait, and ecosystem service database applied to second-generation bioenergy feedstock production. *Global Change Biology Bioenergy*, 10(1), 61–71. https://doi.org/10.1111/gcbb.12420

Leuning, R. (1995). A critical appraisal of a combined stomatal-photosynthesis model for C3 plants. *Plant, Cell & Environment*, 18(4), 339–355. https://doi.org/10.1111/j.1365-3040.1995.tb00370.x

Lin, C., Gentine, P., Huang, Y., Guan, K., Kimm, H., & Zhou, S. (2018). Diel ecosystem conductance response to vapor pressure deficit is suboptimal and independent of soil moisture. *Agricultural and Forest Meteorology*, 250, 24–34. https://doi.org/10.1016/j.agrformet.2017.12.078

Lin, Y.-S., Medlyn, B. E., Duursma, R. A., Prentice, I. C., Wang, H., Baig, S., ... Wingate, L. (2015). Optimal stomatal behaviour around the world. *Nature Climate Change*, 5(5), 459–464. https://doi.org/10.1038/nclimate2550

Liu, J., Bowman, K. W., Schimel, D. S., Parazoo, N. C., Jiang, Z., Lee, M., ... Eldering, A. (2017). Contrasting carbon cycle responses of the tropical continents to the 2015–2016 El Niño. *Science*, 358(6360), 2015–2016. https://doi.org/10.1126/science.aam5690

Lopes, A. P., Nelson, B. W., Wu, J., Graça, P. M. L., Tavares, J. V., Prohaska, N., ... Saleska, S. R. (2016). Leaf flush drives dry season green-up of the Central Amazon. *Remote Sensing of Environment*, 182, 90–98. https://doi.org/10.1016/j.rse.2016.05.009

Martínez-Vilalta, J., Poyatos, R., Aguadé, D., Retana, J., & Mencuccini, M. (2014). A new look at water transport regulation in plants. *New Phytologist*, 204(1), 105–115. https://doi.org/10.1111/nph.12912

McDowell, N., Brooks, J. R., Fitzgerald, S. A., & Bond, B. J. (2003). Carbon isotope discrimination and growth response of old Pinus ponderosa trees to stand density reductions. *Plant, Cell & Environment*, 26(4), 631–644. https://doi.org/10.1046/j.1365-3040.2003.00999.x

Medlyn, B. E., Duursma, R. A., Eamus, D., Ellsworth, D. S., Prentice, I. C., Barton, C. V. M., … Wingate, L. (2011). Reconciling the optimal and empirical approaches to modelling stomatal conductance. *Global Change Biology*, 17(6), 2134–2144. https://doi.org/10.1111/j.1365-2486.2010.02375.x

Medlyn, B. E., Robinson, A. P., Clement, R., & McMurtrie, R. E. (2005). On the validation of models of forest CO_2 exchange using eddy covariance data: Some perils and pitfalls. *Tree Physiology*, 25(7), 839–857. https://doi.org/10.1093/treephys/25.7.839

Medvigy, D., Wofsy, S. C., Munger, J. W., Hollinger, D. Y., & Moorcroft, P. R. (2009). Mechanistic scaling of ecosystem function and dynamics in space and time: Ecosystem Demography model version 2. *Journal of Geophysical Research: Biogeosciences*, 114(G1), G01002. https://doi.org/10.1029/2008JG000812

Meinzer, F. C., Andrade, J. L., Goldstein, G., Holbrook, N. M., Cavelier, J., & Wright, S. J. (1999). Partitioning of soil water among canopy trees in a seasonally dry tropical forest. *Oecologia*, 121(3), 293–301. https://doi.org/10.1007/s004420050931

Meinzer, F. C., James, S. A., Goldstein, G., & Woodruff, D. (2003). Whole-tree water transport scales with sapwood capacitance in tropical forest canopy trees. *Plant, Cell & Environment*, 26(7), 1147–1155. https://doi.org/10.1046/j.1365-3040.2003.01039.x

Michaletz, S. T., Weiser, M. D., McDowell, N. G., Zhou, J., Kaspari, M., Helliker, B. R., & Enquist, B. J. (2016). The energetic and carbon economic origins of leaf thermoregulation. *Nature Plants*, 2(9), https://doi.org/10.1038/nplants.2016.129

Michaletz, S. T., Weiser, M. D., Zhou, J., Kaspari, M., Helliker, B. R., & Enquist, B. J. (2015). Plant thermoregulation: Energetics, trait–environment interactions, and carbon economics. *Trends in Ecology & Evolution*, 30(12), 714–724. https://doi.org/10.1016/j.tree.2015.09.006

Miner, G. L., Bauerle, W. L., & Baldocchi, D. D. (2017). Estimating the sensitivity of stomatal conductance to photosynthesis: A review. *Plant, Cell & Environment*, 40(7), 1214–1238. https://doi.org/10.1111/pce.12871

Nepstad, D. C., de Carvalho, C. R., Davidson, E. A., Jipp, P. H., Lefebvre, P. A., Negreiros, G. H., … Vieira, S. (1994). The role of deep roots in the hydrological and carbon cycles of Amazonian forests and pastures. *Nature*, 372(6507), 666–669.

Niinemets, Ü., Díaz-Espejo, A., Flexas, J., Galmés, J., & Warren, C. R. (2009). Role of mesophyll diffusion conductance in constraining potential photosynthetic productivity in the field. *Journal of Experimental Botany*, 60(8), 2249–2270. https://doi.org/10.1093/jxb/erp036

Nolf, M., Creek, D., Duursma, R., Holtum, J., Mayr, S., & Choat, B. (2015). Stem and leaf hydraulic properties are finely coordinated in three tropical rain forest tree species. *Plant, Cell & Environment*, 38(12), 2652–2661. https://doi.org/10.1111/pce.12581

Oleson, K. W., Lawrence, D. M., Bonan, G. B., Drewniak, B., Huang, M., Koven, C. D., …Thornton, P. E. (2013). Technical description of version 4.5 of the Community Land Model (CLM). *National Center for Atmospheric Research, Technical Note NCAR/TN-503+ STR*, https://doi.org/10.5065/D6RR1W7M

Oleson, K. W., Lawrence, D. M., Gordon, B., Flanner, M. G., Kluzek, E., Peter, J., …Thornton, P. E. (2010). Technical description of version 4.0 of the Community Land Model (CLM). *National Center for Atmospheric Research, Technical Note NCAR/TN-478+STR*, https://doi.org/10.5065/D6FB50WZ

Pantin, F., Simonneau, T., & Muller, B. (2012). Coming of leaf age: Control of growth by hydraulics and metabolics during leaf ontogeny. *New Phytologist*, 196(2), 349–366. https://doi.org/10.1111/j.1469-8137.2012.04273.x

Pielke, R. A., Avissar, R., Raupach, M., Dolman, A. J., Zeng, X., & Denning, A. S. (1998). Interactions between the atmosphere and terrestrial ecosystems: Influence on weather and climate. *Global Change Biology*, 4(5), 461–475. https://doi.org/10.1046/j.1365-2486.1998.t01-1-00176.x

Reyer, C. P. O., Leuzinger, S., Rammig, A., Wolf, A., Bartholomeus, R. P., Bonfante, A., … Pereira, M. (2013). A plant's perspective of extremes: Terrestrial plant responses to changing climatic variability. *Global Change Biology*, 19(1), 75–89. https://doi.org/10.1111/gcb.12023

Rodriguez-Dominguez, C. M., Buckley, T. N., Egea, G., de Cires, A., Hernandez-Santana, V., Martorell, S., & Diaz-Espejo, A. (2016). Most stomatal closure in woody species under moderate drought can be explained by stomatal responses to leaf turgor. *Plant, Cell & Environment*, 39(9), 2014–2026. https://doi.org/10.1111/pce.12774

Rogers, A., McDonald, K., Muehlbauer, M. F., Hoffman, A., Koenig, K., Newman, L., … Lelie, D. (2012). Inoculation of hybrid poplar with the endophytic bacterium *Enterobacter* sp 638 increases biomass but does not impact leaf level physiology. *Global Change Biology Bioenergy*, 4(3), 364–370. https://doi.org/10.1111/j.1757-1707.2011.01119.x

Rogers, A., Medlyn, B. E., Dukes, J. S., Bonan, G., Caemmerer, S., Dietze, M. C., … Zaehle, S. (2017). A roadmap for improving the representation of photosynthesis in Earth system models. *New Phytologist*, 213(1), 22–42. https://doi.org/10.1111/nph.14283

Rogers, A., Serbin, S. P., Ely, K. S., Sloan, V. L., & Wullschleger, S. D. (2017). Terrestrial biosphere models underestimate photosynthetic capacity and CO_2 assimilation in the Artic. *New Phytologist*, 216(4), 1090–1103.

Rogers, A., Serbin, S., Ely, K., Wu, J., Wolfe, B., Dickman, T., …Michaletz, S. (2018a). Diurnal leaf gas exchange survey, Feb2016-May2016, PA-SLZ, PA-PNM: Panama. NGEE Tropics Data Collection, https://doi.org/10.15486/ngt/1411972

Rogers, A., Serbin, S., Ely, K., Wu, J., Wolfe, B., Dickman, T., …Michaletz, S. (2018b). CO_2 response (ACi) gas exchange, calculated Vcmax & Jmax parameters, Feb2016-May2016, PA-SLZ, PA-PNM: Panama. NGEE Tropics Data Collection, https://doi.org/10.15486/ngt/1411867

Serbin, S. P., Singh, A., McNeil, B. E., Kingdon, C. C., & Townsend, P. A. (2014). Spectroscopic determination of leaf morphological and biochemical traits for northern temperate and boreal tree species. *Ecological Applications*, 24(7), 1651–1669. https://doi.org/10.1890/13-2110.1

Singh, A., Serbin, S. P., McNeil, B. E., Kingdon, C. C., & Townsend, P. A. (2015). Imaging spectroscopy algorithms for mapping canopy foliar chemical and morphological traits and their uncertainties. *Ecological Applications*, 25(8), 2180–2197. https://doi.org/10.1890/14-2098.1

Sitch, S., Smith, B., Prentice, I. C., Arneth, A., Bondeau, A., Cramer, W., … Venevsky, S. (2003). Evaluation of ecosystem dynamics, plant geography and terrestrial carbon cycling in the LPJ dynamic global vegetation model. *Global Change Biology*, 9(2), 161–185. https://doi.org/10.1046/j.1365-2486.2003.00569.x

Sperry, J. S., Venturas, M. D., Anderegg, W. R., Mencuccini, M., Mackay, D. S., Wang, Y., & Love, D. M. (2017). Predicting stomatal responses to the environment from the optimization of photosynthetic gain and hydraulic cost. *Plant, Cell & Environment*, 40(6), 816–830. https://doi.org/10.1111/pce.12852

Stavros, E. N., Schimel, D., Pavlick, R., Serbin, S., Swann, A., Duncanson, L., … Wennberg, P. (2017). ISS observations offer insights into plant function. *Nature Ecology and Evolution*, 1(7), https://doi.org/10.1038/s41559-017-0194

Sun, Y., Gu, L., Dickinson, R. E., Norby, R. J., Pallardy, S. G., & Hoffman, F. M. (2014). Impact of mesophyll diffusion on estimated global land CO_2 fertilization. *Proceedings of the National Academy of Sciences of the United States of America*, 111(44), 15774–15779. https://doi.org/10.1073/pnas.1418075111

Terashima, I., Miyazawa, S. I., & Hanba, Y. T. (2001). Why are sun leaves thicker than shade leaves?—Consideration based on analyses of CO_2 diffusion in the leaf. *Journal of Plant Research*, 114(1), 93–105. https://doi.org/10.1007/PL00013972

Tuzet, A., Perrier, A., & Leuning, R. (2003). A coupled model of stomatal conductance, photosynthesis and transpiration. *Plant Cell & Environment*, 26(7), 1097–1116. https://doi.org/10.1046/j.1365-3040.2003.01035.x

Venturas, M. D., Sperry, J. S., Love, D. M., Frehner, E. H., Allred, M. G., Wang, Y., & Anderegg, W. R. (2018). A stomatal control model based on optimization of carbon gain versus hydraulic risk predicts aspen sapling responses to drought. *New Phytologist*, 220(3), 836–850. https://doi.org/10.1111/nph.15333

Williams, M., Rastetter, E. B., Fernandes, D. N., Goulden, M. L., Wofsy, S. C., Shaver, G. R., … Nadelhoffer, K. J. (1996). Modelling the soil-plant-atmosphere continuum in a Quercus-Acer stand at Harvard forest: The regulation of stomatal conductance by light, nitrogen and soil/plant hydraulic properties. *Plant Cell & Environment*, 19(8), 911–927. https://doi.org/10.1111/j.1365-3040.1996.tb00456.x

Wolf, A., Anderegg, W. R., & Pacala, S. W. (2016). Optimal stomatal behavior with competition for water and risk of hydraulic impairment. *Proceedings of the National Academy of Sciences of the United States of America*, 113(46), E7222–E7230. https://doi.org/10.1073/pnas.1615144113

Wolfe, B. T., Sperry, J. S., & Kursar, T. A. (2016). Does leaf shedding protect stems from cavitation during seasonal droughts? A test of the hydraulic fuse hypothesis. *New Phytologist*, 212(4), 1007–1018. https://doi.org/10.1111/nph.14087

Wolfe, B., Wu, J., Ely, K., Serbin, S., Rogers, A., Dickman, T., …Michaletz, S. (2018). Leaf water potential, Feb2016-May2016, PA-SLZ, PA-PNM, PA-BCI: Panama. NGEE Tropics Data Collection, https://doi.org/10.15486/ngt/1411970

Wolz, K. J., Wertin, T. M., Abordo, M., Wang, D., & Leakey, A. D. (2017). Diversity in stomatal function is integral to modelling plant carbon and water fluxes. *Nature Ecology & Evolution*, 1, 1292–1298. https://doi.org/10.1038/s41559-017-0238-z

Wright, I. J., Reich, P. B., Westoby, M., Ackerly, D. D., Baruch, Z., Bongers, F., … Villar, R. (2004). The worldwide leaf economics spectrum. *Nature*, 428(6985), 821–827.

Wright, J. S., Fu, R., Worden, J. R., Chakraborty, S., Clinton, N. E., Risi, C., … Yin, L. (2017). Rainforest-initiated wet season onset over the southern Amazon. *Proceedings of the National Academy of Sciences of the United States of America*, 114(32), 8481–8486. https://doi.org/10.1073/pnas.1621516114

Wright, S. J., Horlyck, V., Basset, Y., Barrios, H., Bethancourt, A., Bohlman, S. A., … Zotz, G. (2003). Tropical canopy biology program, Republic of Panama. In Y. Basset, V. Horlyck, & S. J. Wright (Eds.), *Studying forest canopies from above: The international canopy crane network* (pp. 137–155). Panama City, Panama: Smithsonian Tropical Research Institute and the United Nations Environmental Programme.

Wright, S. J., Kitajima, K., Kraft, N. J., Reich, P. B., Wright, I. J., Bunker, D. E., … Zanne, A. E. (2010). Functional traits and the growth-mortality tradeoff in tropical trees. *Ecology*, 91(12), 3664–3674. https://doi.org/10.1890/09-2335.1

Wu, J., Albert, L. P., Lopes, A. P., Restrepo-Coupe, N., Hayek, M., Wiedemann, K. T., … Saleska, S. R. (2016). Leaf development and demography explain photosynthetic seasonality in Amazon evergreen forests. *Science*, 351(6276), 972–976. https://doi.org/10.1126/science.aad5068

Wu, J., Kobayashi, H., Stark, S. C., Meng, R., Guan, K., Tran, N. N., … Saleska, S. R. (2018). Biological processes dominate seasonality of remotely sensed canopy greenness in an Amazon evergreen forest. *New Phytologist*, 217(4), 1507–1520. https://doi.org/10.1111/nph.14939

Xu, L., & Baldocchi, D. D. (2003). Seasonal trends in photosynthetic parameters and stomatal conductance of blue oak (*Quercus douglasii*) under prolonged summer drought and high temperature. *Tree Physiology*, 23(13), 865–877. https://doi.org/10.1093/treephys/23.13.865

Xu, X., Medvigy, D., Powers, J. S., Becknell, J. M., & Guan, K. (2016). Diversity in plant hydraulic traits explains seasonal and inter-annual variations of vegetation dynamics in seasonally dry tropical forests. *New Phytologist*, 212(1), 80–95. https://doi.org/10.1111/nph.14009

Zeng, Z., Piao, S., Li, L. Z., Zhou, L., Ciais, P., Wang, T., … Wang, Y. (2017). Climate mitigation from vegetation biophysical feedbacks during the past three decades. *Nature Climate Change*, 7(6), 432–436. https://doi.org/10.1038/nclimate3299

Zhou, S. X., Medlyn, B. E., & Prentice, I. C. (2015). Long-term water stress leads to acclimation of drought sensitivity of photosynthetic capacity in xeric but not riparian Eucalyptus species. *Annals of Botany*, 117(1), 133–144.

Zhou, S., Medlyn, B., Sabaté, S., Sperlich, D., Prentice, I. C., & Whitehead, D. (2014). Short-term water stress impacts on stomatal, mesophyll and biochemical limitations to photosynthesis differ consistently among tree species from contrasting climates. *Tree Physiology*, 34(10), 1035–1046. https://doi.org/10.1093/treephys/tpu072

SUPPORTING INFORMATION

Additional supporting information may be found online in the Supporting Information section at the end of the article.